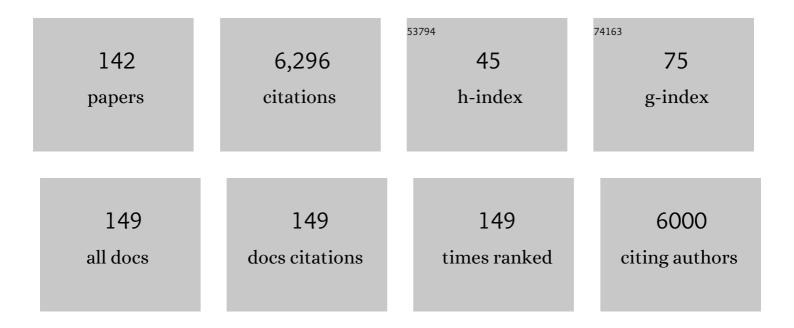
List of Publications by Year in descending order

Source: https://exaly.com/author-pdf/2876428/publications.pdf Version: 2024-02-01



#	Article	IF	CITATIONS
1	Correction of motional artifacts in diffusion-weighted MR images using navigator echoes. Magnetic Resonance Imaging, 1994, 12, 455-460.	1.8	329
2	Assessment of relative brain iron concentrations using <i>T</i> ₂ â€weighted and <i>T</i> ₂ *â€weighted MRI at 3 Tesla. Magnetic Resonance in Medicine, 1994, 32, 335-341.	3.0	317
3	Increased ironâ€related MRI contrast in the substantia nigra in Parkinson's disease. Neurology, 1995, 45, 1138-1143.	1.1	300
4	High field MRI correlates of myelin content and axonal density in multiple sclerosis. Journal of Neurology, 2003, 250, 1293-1301.	3.6	266
5	Magnetic resonance imaging assessment of evolving focal cerebral ischemia. Comparison with histopathology in rats Stroke, 1994, 25, 1252-1261.	2.0	253
6	Cerebral quantitative susceptibility mapping predicts amyloid-Î ² -related cognitive decline. Brain, 2017, 140, 2112-2119.	7.6	213
7	Temporal evolution of ischemic damage in rat brain measured by proton nuclear magnetic resonance imaging Stroke, 1991, 22, 802-808.	2.0	195
8	Frequency offset corrected inversion (FOCI) pulses for use in localized spectroscopy. Magnetic Resonance in Medicine, 1996, 36, 562-566.	3.0	189
9	Real-time movie imaging from a single cardiac cycle by NMR. Magnetic Resonance in Medicine, 1987, 5, 246-254.	3.0	144
10	High field (9.4 Tesla) magnetic resonance imaging of cortical grey matter lesions in multiple sclerosis. Brain, 2010, 133, 858-867.	7.6	138
11	Early changes in water diffusion, perfusion, T1, and T2 during focal cerebral ischemia in the rat studied at 8.5 T. Magnetic Resonance in Medicine, 1999, 41, 479-485.	3.0	130
12	Improvements in snap-shot nuclear magnetic resonance imaging. British Journal of Radiology, 1988, 61, 822-828.	2.2	122
13	The measurement of diffusion and perfusion in biological systems using magnetic resonance imaging. Physics in Medicine and Biology, 2000, 45, R97-R138.	3.0	112
14	High-speed multisliceT1mapping using inversion-recovery echo-planar imaging. Magnetic Resonance in Medicine, 1990, 16, 238-245.	3.0	98
15	Whole-body echo-planar MR imaging at 0.5 T Radiology, 1989, 170, 257-263.	7.3	93
16	Histopathological correlations of nuclear magnetic resonance imaging parameters in experimental cerebral ischemia. Magnetic Resonance Imaging, 1993, 11, 241-246.	1.8	92
17	Use of Mitochondrial Inhibitors to Demonstrate That Cytochrome Oxidase Near-Infrared Spectroscopy Can Measure Mitochondrial Dysfunction Noninvasively in the Brain. Journal of Cerebral Blood Flow and Metabolism, 1999, 19, 27-38.	4.3	91
18	Feasibility of simultaneous intracranial EEG-fMRI in humans: A safety study. NeuroImage, 2010, 49, 379-390.	4.2	85

#	Article	IF	CITATIONS
19	Temporal evolution and spatial distribution of the diffusion constant of water in rat brain after transient middle cerebral artery occlusion. Journal of the Neurological Sciences, 1993, 120, 123-130.	0.6	78
20	Anisotropic water diffusion in white and gray matter of the neonatal piglet brain before and after transient hypoxia-ischaemia. Magnetic Resonance Imaging, 1997, 15, 433-440.	1.8	77
21	Echo planar imaging of the human fetus <i>in utero</i> at 0.5 T. British Journal of Radiology, 1990, 63, 833-841.	2.2	74
22	The Effect of Hypothermia on Transient Focal Ischemia in Rat Brain Evaluated by Diffusion- and Perfusion-Weighted NMR Imaging. Journal of Cerebral Blood Flow and Metabolism, 1994, 14, 732-741.	4.3	74
23	Temporal and anatomical variations of brain water apparent diffusion coefficient in perinatal cerebral hypoxic-ischemic injury: Relationships to cerebral energy metabolism. Magnetic Resonance in Medicine, 1998, 39, 920-927.	3.0	73
24	Behavioral, blood and magnetic resonance imaging biomarkers of experimental mild traumatic brain injury. Scientific Reports, 2016, 6, 28713.	3.3	72
25	MRI measurements of cerebral deoxyhaemoglobin concentration [dHb]—correlation with near infrared spectroscopy (NIRS). , 1998, 11, 281-289.		70
26	Acute elevation and recovery of intracellular [Mg ²⁺] following human focal cerebral ischemia. Neurology, 1993, 43, 1577-1577.	1.1	70
27	Real-time flow measurements using echo-planar imaging. Magnetic Resonance in Medicine, 1991, 18, 1-8.	3.0	68
28	Implementation of quantitative FAIR perfusion imaging with a short repetition time in time-course studies. Magnetic Resonance in Medicine, 1999, 41, 829-840.	3.0	68
29	Depth of delayed cooling alters neuroprotection pattern after hypoxia-ischemia. Annals of Neurology, 2005, 58, 75-87.	5.3	62
30	Delayed Whole-Body Cooling to 33 or 35ÂC and the Development of Impaired Energy Generation Consequential to Transient Cerebral Hypoxia-Ischemia in the Newborn Piglet. Pediatrics, 2006, 117, 1549-1559.	2.1	59
31	Role of the human supplementary eye field in the control of saccadic eye movements. Neuropsychologia, 2007, 45, 997-1008.	1.6	59
32	In vivo hadamard encoded continuous arterial spin labeling (H-CASL). Magnetic Resonance in Medicine, 2010, 63, 1111-1118.	3.0	58
33	Snapshot imaging at 0.5 t using echo-planar techniques. Magnetic Resonance in Medicine, 1989, 10, 227-240.	3.0	57
34	Magnetic resonance virtual histology for embryos: 3D atlases for automated high-throughput phenotyping. Neurolmage, 2011, 54, 769-778.	4.2	57
35	Rapid biomedical imaging by NMR. British Journal of Radiology, 1981, 54, 850-855.	2.2	55
36	Investigation of cerebral ischemia using magnetization transfer contrast (MTC) MR imaging. Magnetic Resonance Imaging, 1991, 9, 895-902.	1.8	55

#	Article	IF	CITATIONS
37	Changes in Apparent Fiber Density and Track-Weighted Imaging Metrics in White Matter following Experimental Traumatic Brain Injury. Journal of Neurotrauma, 2017, 34, 2109-2118.	3.4	55
38	High resolution MRI of the brain at 4.7â€Tesla using fast spin echo imaging. British Journal of Radiology, 2003, 76, 631-637.	2.2	53
39	High-resolution fast spin echo imaging of the human brain at 4.7 T: Implementation and sequence characteristics. Magnetic Resonance in Medicine, 2004, 51, 1254-1264.	3.0	53
40	A general approach to selection of multiple cubic volume elements using the ISIS technique. Magnetic Resonance in Medicine, 1988, 8, 323-331.	3.0	52
41	Snapshot head imaging at 0.5 T using the echo planar technique. Magnetic Resonance in Medicine, 1988, 8, 110-115.	3.0	50
42	A quantitative method for fast diffusion imaging using magnetization-prepared turboFLASH. Magnetic Resonance in Medicine, 1998, 39, 950-960.	3.0	50
43	Regional Variation of Cerebral Blood Flow and Arterial Transit Time in the Normal and Hypoperfused Rat Brain Measured Using Continuous Arterial Spin Labeling MRI. Journal of Cerebral Blood Flow and Metabolism, 2006, 26, 274-282.	4.3	50
44	Traumatic Brain Injury Results in Cellular, Structural and Functional Changes Resembling Motor Neuron Disease. Cerebral Cortex, 2017, 27, 4503-4515.	2.9	50
45	Study of internal structure of the human fetus in utero by echo-planar magnetic resonance imaging. American Journal of Obstetrics and Gynecology, 1990, 163, 601-607.	1.3	47
46	REAL-TIME CARDIAC IMAGING OF ADULTS AT VIDEO FRAME RATES BY MAGNETIC RESONANCE IMAGING. Lancet, The, 1986, 328, 682.	13.7	46
47	PEEP—A rapid chemical-shift imaging method. Magnetic Resonance in Medicine, 1989, 10, 282-287.	3.0	46
48	Comparative Prognostic Utilities of Early Quantitative Magnetic Resonance Imaging Spin-Spin Relaxometry and Proton Magnetic Resonance Spectroscopy in Neonatal Encephalopathy. Pediatrics, 2006, 118, 1467-1477.	2.1	45
49	Zonally magnified EPI in real time by NMR. Journal of Physics E: Scientific Instruments, 1988, 21, 275-280.	0.7	43
50	Acute changes in MRI diffusion, perfusion,T1, andT2 in a rat model of oligemia produced by partial occlusion of the middle cerebral artery. Magnetic Resonance in Medicine, 2000, 44, 706-712.	3.0	42
51	Volume Selection Using Gradients and Selective Pulses. Annals of the New York Academy of Sciences, 1987, 508, 376-385.	3.8	40
52	Random noise selective excitation pulses. Magnetic Resonance in Medicine, 1987, 5, 93-98.	3.0	39
53	Echo-planar imaging of the human fetus in utero. Magnetic Resonance in Medicine, 1990, 13, 314-318.	3.0	39
54	Velocity-driven adiabatic fast passage for arterial spin labeling: Results from a computer model. Magnetic Resonance in Medicine, 2003, 49, 398-401.	3.0	37

#	Article	lF	CITATIONS
55	Inversion-recovery echo-planar imaging (ir-epi) at 0.5 T. Magnetic Resonance in Medicine, 1990, 13, 514-517.	3.0	36
56	Anodal transcranial direct current stimulation increases brain intracellular pH and modulates bioenergetics. International Journal of Neuropsychopharmacology, 2013, 16, 1695-1706.	2.1	36
57	Cardiac arterial spin labeling using segmented ECGâ€gated Look‣ocker FAIR: Variability and repeatability in preclinical studies. Magnetic Resonance in Medicine, 2013, 69, 238-247.	3.0	35
58	Volumar imaging using NMR spin echoes: echo-volumar imaging (EVI) at 0.1 T. Journal of Physics E: Scientific Instruments, 1989, 22, 324-330.	0.7	33
59	3D MDEFT imaging of the human brain at 4.7 T with reduced sensitivity to radiofrequency inhomogeneity. Magnetic Resonance in Medicine, 2005, 53, 1452-1458.	3.0	33
60	Cardiac phenotyping in <i>ex vivo</i> murine embryos using <i>µ</i> MRI. NMR in Biomedicine, 2009, 22, 857-866.	2.8	33
61	Characterizing the Origin of the Arterial Spin Labelling Signal in MRI Using a Multiecho Acquisition Approach. Journal of Cerebral Blood Flow and Metabolism, 2009, 29, 1836-1845.	4.3	33
62	REAL-TIME NMR IMAGING OF CORONARY VESSELS. Lancet, The, 1987, 330, 964-965.	13.7	28
63	Technical challenges of functional magnetic resonance imaging. IEEE Engineering in Medicine and Biology Magazine, 2000, 19, 42-54.	0.8	28
64	Design, construction and evaluation of an anthropomorphic head phantom with realistic susceptibility artifacts. Journal of Magnetic Resonance Imaging, 2007, 26, 202-207.	3.4	28
65	Structural correlates of active-staining following magnetic resonance microscopy in the mouse brain. NeuroImage, 2011, 56, 974-983.	4.2	28
66	7T-fMRI: Faster temporal resolution yields optimal BOLD sensitivity for functional network imaging specifically at high spatial resolution. Neurolmage, 2018, 164, 214-229.	4.2	27
67	BOdependence of the on-resonance longitudinal relaxation time in the rotating frame (T1i) in protein phantoms and rat brain in vivo. Magnetic Resonance in Medicine, 2004, 51, 4-8.	3.0	26
68	Cerebral tissue water spin-spin relaxation times in human neonates at 2.4 Tesla: Methodology and the effects of maturation. Magnetic Resonance Imaging, 1999, 17, 1289-1295.	1.8	25
69	Diffusion tensor parameters and principal eigenvector coherence: Relation to b-value intervals and field strength. Magnetic Resonance Imaging, 2013, 31, 742-747.	1.8	24
70	Simultaneous noninvasive measurement of CBF and CBV using double-echo FAIR (DEFAIR). Magnetic Resonance in Medicine, 2001, 45, 853-863.	3.0	23
71	MR image-guided investigation of regional signal transducers and activators of transcription-1 activation in a rat model of focal cerebral ischemia. Neuroscience, 2004, 127, 333-339.	2.3	23
72	Spin-echo MRS in humans at high field: LASER localisation using FOCI pulses. Journal of Magnetic Resonance, 2005, 175, 30-43.	2.1	23

#	Article	IF	CITATIONS
73	Improving whole brain structural MRI at 4.7 Tesla using 4 irregularly shaped receiver coils. NeuroImage, 2006, 32, 1176-1184.	4.2	23
74	In vivo measurement of the longitudinal relaxation time of arterial blood (T1a) in the mouse using a pulsed arterial spin labeling approach. Magnetic Resonance in Medicine, 2006, 55, 943-947.	3.0	23
75	Assessment of magnetic field (4.7 T) induced forces on prosthetic heart valves and annuloplasty rings. Journal of Magnetic Resonance Imaging, 2005, 22, 311-317.	3.4	22
76	Atraumatic quantitation of cerebral perfusion in cats by19f magnetic resonance imaging. Magnetic Resonance in Medicine, 1992, 28, 39-53.	3.0	21
77	EPI distortion correction from a simultaneously acquired distortion map using TRAIL. Journal of Magnetic Resonance Imaging, 2006, 23, 597-603.	3.4	21
78	3Dâ€multiâ€echo radial imaging of ²³ Na (3Dâ€MERINA) for timeâ€efficient multiâ€parameter tissue compartment mapping. Magnetic Resonance in Medicine, 2018, 79, 1950-1961.	² 3.0	21
79	Correlation between Absolute Deoxyhaemoglobin [dHb] Measured by Near Infrared Spectroscopy (NIRS) and Absolute R2′ as Determined by Magnetic Resonance Imaging (MRI). Advances in Experimental Medicine and Biology, 1997, 413, 129-137.	1.6	21
80	Ultrafast magnetic resonance scanning of the liver with echo-planar imaging. British Journal of Radiology, 1990, 63, 430-437.	2.2	20
81	Observation of cerebrospinal fluid flow with echo-planar magnetic resonance imaging. British Journal of Radiology, 1991, 64, 89-97.	2.2	19
82	Comparative Study of the FAIR Technique of Perfusion Quantification with the Hydrogen Clearance Method. Journal of Cerebral Blood Flow and Metabolism, 2003, 23, 689-699.	4.3	19
83	Magnetic resonance proton spectroscopy and diffusion weighted imaging of chick embryo brain in ovo. Developmental Brain Research, 2003, 141, 101-107.	1.7	18
84	Measurement of T1by echo-planar imaging and the construction of computer-generated images. Physics in Medicine and Biology, 1986, 31, 113-124.	3.0	16
85	ECHO-PLANAR MAGNETIC RESONANCE IMAGING IN ABNORMAL PREGNANCIES. Lancet, The, 1989, 334, 157.	13.7	16
86	Rapid Simultaneous Mapping of T2 and T2* by Multiple Acquisition of Spin and Gradient Echoes Using Interleaved Echo Planar Imaging (MASAGE-IEPI). NeuroImage, 2002, 15, 992-1002.	4.2	16
87	Multislice cardiac arterial spin labeling using improved myocardial perfusion quantification with simultaneously measured blood pool input function. Magnetic Resonance in Medicine, 2013, 70, 1125-1136.	3.0	16
88	Active detune switch for complete sensitive-volume localization in in Vivo spectroscopy using multiple rf coils and depth pulses. Journal of Magnetic Resonance, 1984, 60, 473-478.	0.5	15
89	Delayed hypothermia prevents decreases in N-acetylaspartate and reduced glutathione in the cerebral cortex of the neonatal pig following transient hypoxia-ischaemia. Neurochemical Research, 2002, 27, 1599-1604.	3.3	15
90	TurboFLASH FAIR imaging with optimized inversion and imaging profiles. Magnetic Resonance in Medicine, 2004, 51, 46-54.	3.0	15

#	Article	IF	CITATIONS
91	Mapping somatosensory connectivity in adult mice using diffusion MRI tractography and super-resolution track density imaging. NeuroImage, 2014, 102, 381-392.	4.2	15
92	Using the robust principal component analysis algorithm to remove RF spike artifacts from MR images. Magnetic Resonance in Medicine, 2016, 75, 2517-2525.	3.0	15
93	Reperfusion in a Cerbil Model of Forebrain Ischemia Using Serial Magnetic Resonance FAIR Perfusion Imaging. Stroke, 1999, 30, 1263-1270.	2.0	14
94	Understanding and optimizing the amplitude modulated control for multiple-slice continuous arterial spin labeling. Magnetic Resonance in Medicine, 2005, 54, 594-604.	3.0	14
95	1H Magnetic Resonance Imaging of Normal Brain Tissue Response to Photodynamic Therapy. Neurosurgery, 1991, 29, 538-543.	1.1	13
96	Magnetization transfer contrast (MTC) in FLASH MR imaging. Magnetic Resonance Imaging, 1991, 9, 889-893.	1.8	13
97	Greater Hypoxia-Induced Cell Death in Prenatal Brain after Bacterial-Endotoxin Pretreatment is not Because of Enhanced Cerebral Energy Depletion: A Chicken Embryo Model of the Intrapartum Response to Hypoxia and Infection. Journal of Cerebral Blood Flow and Metabolism, 2008, 28, 948-960.	4.3	12
98	Rapid T2* mapping using interleaved echo planar imaging. Magnetic Resonance in Medicine, 1999, 41, 368-374.	3.0	11
99	Translational and rotational forces on heart valve prostheses subjected ex vivo to a 4.7-T MR system. Journal of Magnetic Resonance Imaging, 2002, 16, 653-659.	3.4	11
100	Magnetic Resonance Imaging of Neonatal Encephalopathy at 4.7 Tesla: Initial Experiences. Pediatrics, 2006, 118, e1812-e1821.	2.1	11
101	Quantifying the area-at-risk of myocardial infarction in-vivo using arterial spin labeling cardiac magnetic resonance. Scientific Reports, 2017, 7, 2271.	3.3	11
102	3D DT-MRI using a reduced-FOV approach and saturation pulses. Magnetic Resonance in Medicine, 2004, 51, 853-857.	3.0	10
103	Method for spatially interleaving two images to halve EPI readout times: Two reduced acquisitions interleaved (TRAIL). Magnetic Resonance in Medicine, 2004, 51, 1212-1222.	3.0	10
104	Human Whole Body Line Scan Imaging by Nuclear Magnetic Resonance. IEEE Transactions on Nuclear Science, 1979, 26, 2817-2820.	2.0	7
105	Common SENSE (sensitivity encoding using hardware common to all MR scanners): A new method for single-shot segmented echo planar imaging. Magnetic Resonance in Medicine, 2005, 54, 402-410.	3.0	7
106	Monitoring systemic amyloidosis using MRI measurements of the extracellular volume fraction. Amyloid: the International Journal of Experimental and Clinical Investigation: the Official Journal of the International Society of Amyloidosis, 2013, 20, 93-98.	3.0	7
107	Preliminary observations of transverse relaxation rates obtained at 3 Tesla from the substantia nigra of adult normal human brain. NMR in Biomedicine, 1995, 8, 25-27.	2.8	6
108	Selective averaging for the diffusion tensor measurement. Magnetic Resonance Imaging, 2005, 23, 585-590.	1.8	6

#	Article	IF	CITATIONS
109	Gradual changes in the apparent diffusion coefficient of water in selectively vulnerable brain regions following brief ischemia in the gerbil. Magnetic Resonance in Medicine, 2005, 53, 593-600.	3.0	6
110	Reducing ghosting due to k-space discontinuities in fast spin echo (FSE) imaging by a new combination of k-space ordering and parallel imaging. Journal of Magnetic Resonance, 2009, 200, 119-125.	2.1	5
111	A low flip angle spin-echo technique for producing rapid diffusion weighted MR images. Magnetic Resonance Imaging, 1994, 12, 727-731.	1.8	4
112	Feasibility of identifying the ideal locations for motor intention decoding using unimodal and multimodal classification at 7T-fMRI. Scientific Reports, 2018, 8, 15556.	3.3	4
113	236 Non-Invasive Cerebral Temperature Mapping by Proton Spectroscopic Imaging. Pediatric Research, 2004, 56, 504-504.	2.3	3
114	Subpixel Enhancement of Nonuniform Tissue (SPENT): A Novel MRI Technique for Quantifying BMD. Journal of Bone and Mineral Research, 2009, 24, 324-333.	2.8	3
115	Micro-MRI phenotyping of a novel double-knockout mouse model of congenital heart disease. Journal of Cardiovascular Magnetic Resonance, 2010, 12, .	3.3	3
116	Diffusion microscopic MRI of the mouse embryo: Protocol and practical implementation in the <i>splotch</i> mouse model. Magnetic Resonance in Medicine, 2015, 73, 731-739.	3.0	3
117	Relative assessment of brain iron levels using MRI at 3 tesla. Magnetic Resonance Materials in Physics, Biology, and Medicine, 1994, 2, 449-450.	2.0	2
118	Letter to the Editor. Journal of Magnetic Resonance Imaging, 1999, 9, 630-630.	3.4	2
119	NMR investigation of the nature of water in disposable incontinence pads containing superabsorbent polymers and fluffed wood pulp. Colloid and Polymer Science, 2003, 281, 1127-1135.	2.1	2
120	Equilibrium contrast CMR for the detection of amyloidosis in mice. Journal of Cardiovascular Magnetic Resonance, 2011, 13, .	3.3	2
121	Ultraâ€highâ€field MRI using composite RF (STEP) pulses. NMR in Biomedicine, 2021, 34, e4445.	2.8	2
122	MRI safety limits: is MRI safe or not?. British Journal of Radiology, 2000, 73, 1-2.	2.2	2
123	4509015 Nuclear magnetic resonance methods. Magnetic Resonance Imaging, 1986, 4, III-IV.	1.8	1
124	Global Call to Action on MR Safety. Journal of Magnetic Resonance Imaging, 1999, 9, 629-629.	3.4	1
125	118 Delayed Hypoyhermia is Neuroprotective in Moderate, but not Severe, Perinatal Hypoxic-Ischaemic Brain Injury. Pediatric Research, 2004, 56, 484-484.	2.3	1
126	269 Secondary Energy Failure in a Model of Hypoxic Ischaemic Brain Injury Assessed by Serial Phosphorous Magnetic Resonance Spectroscopy, Water Apparent Diffusion and Electrophysiology: A Pilot Study. Pediatric Research, 2004, 56, 509-509.	2.3	1

#	Article	IF	CITATIONS
127	416 Cerebral Alanine Increases During the Evolution of Secondary Energy Failure Following Transient Hypoxia-Ischaemia in Newborn Brain. Pediatric Research, 2005, 58, 426-426.	2.3	1
128	Localized 4.7 T Proton Magnetic Resonance Spectroscopy in Neonatal Encephalopathy: Implementation, Safety and Preliminary Interpretation of Results. Imaging Decisions (Berlin, Germany), 2005, 9, 31-41.	0.2	1
129	Doubling the resolution of echo-planar brain imaging by acquisition of two k-space lines per gradient reversal using TRAIL. NMR in Biomedicine, 2008, 21, 79-88.	2.8	1
130	Improved cardiac arterial spin labelling in the mouse heart by optimisation of acquisition and analysis. Journal of Cardiovascular Magnetic Resonance, 2011, 13, .	3.3	1
131	NMR imaging. , 1980, , 453-462.		1
132	Volume Selection Strategies for In Vivo Biological Spectroscopy. , 1986, , 105-117.		1
133	The Investigation of Structure and Metabolism by In Vivo NMR. , 1985, , 519-522.		1
134	4714883 Method and apparatus for obtaining localized NMR spectra. Magnetic Resonance Imaging, 1988, 6, VI.	1.8	0
135	4906932 NMR spectroscopy and NMR imaging. Magnetic Resonance Imaging, 1991, 9, X.	1.8	0
136	Image Guided Volume Selective Spectroscopy: A Comparison of Techniques for In-Vivo 31P NMR Spectroscopy of Human Brain. Nmr, 1992, , 103-117.	0.5	0
137	The regulation of MR examinations in Germany: a threat to scientific and technical progress for MR in Europe?. Magnetic Resonance Materials in Physics, Biology, and Medicine, 2000, 10, 4-5.	2.0	0
138	85 Initial Experiences of Magnetic Resonance Imaging and Spectroscopy of the Newborn Brain At 4.7 Tesla. Pediatric Research, 2005, 58, 369-369.	2.3	0
139	Accuracy of infarct measurements by inversion recovery delayed-enhancement MRI during the hyper-acute phase of myocardial infarction in rats. Journal of Cardiovascular Magnetic Resonance, 2010, 12, .	3.3	0
140	Snapshot Magnetic Resonance Imaging In Adults. , 1988, , 377-377.		0
141	Changes in the Biophysical Environment of Water Following Focal Brain Ischemia in the Rat. , 1994, , 36-48.		Ο
142	Ultrahigh field brain magnetic resonance imaging using semiadiabatic radiofrequency pulses. NMR in Biomedicine, 2021, , e4672.	2.8	0